Astron. Nachr./AN **323** (2002) 1, 21–30

Light–induced drift for Hg isotopes in chemically peculiar stars

A. ARET AND A. SAPAR

Tartu Observatory, 61602 Tõravere, Estonia

Received 2001 June 24; accepted 2001 December 15

Abstract. In the present paper the abundance anomalies of mercury and its isotopes in the atmospheres of HgMn stars have been studied. Observations have shown strongly anomalous isotopic composition of Hg, Pt, Tl and He in the atmospheres of such CP stars. Generation of elemental abundance anomalies in quiescent atmospheres of CP stars can generally be explained by the mechanism of diffusive segregation of elements due to oppositely directed gravitational and radiative forces. It has been shown that the formation of the observed isotopic anomalies can be successfully explained by a diffusion mechanism called the light–induced drift (LID). The observed ratios of isotopes also enable to estimate the evolutionary stages of CP stars.

Key words: stars: atmospheres — stars: abundances — stars: chemically peculiar

1. Introduction

Elemental abundances of about 15 % of the atmospheres of main sequence stars of the spectral classes B5–F5 are anomalous. The generation of these anomalies in quiescent atmospheres of CP (chemically peculiar) stars is ascribed to elemental diffusion due to radiative acceleration resulting from the transfer of photon momentum to atomic particles in the photon absorption processes dominantly in the spectral line profiles. This effect was first studied in detail by Michaud (1970). The HgMn stars have T_{eff} between 10 000 and 16 000 K, low rotational velocities (Wolff & Preston 1978) and weak or non-existent magnetic fields in their atmospheres (Smith 1996a).

The abundance anomalies include overabundances of manganese, strontium, platinum, mercury, gallium, etc., and at the same time underabundances of aluminium, nickel, cobalt, zinc, etc. (Smith & Dworetsky 1993; Smith 1993, 1994, 1996a, 1996b, 1997). Recent observations show strongly anomalous isotopic composition for Hg, Pt, Tl (overabundancy of heavier isotopes) and He (overabundancy of ^{3}He) (Cowley & Aikman 1975; Kalus et al. 1998; Leckrone et al. 1996; Proffitt et al. 1999; White et al. 1976). In the present paper we analyze the generation of isotopic anomalies for mercury in the atmospheres of mercury–manganese (HgMn) stars due to light–induced drift, radiative force and gravity.

The adopted stellar parameters, elemental abundances and isotopic composition for MnHg stars χ Lup and HR7775 are given in Table 1 as an example (Adelman 1994; Jomaron, Dworetsky & Bohlender 1998; Kalus et al. 1998; Smith & Dworetsky 1993; Wahlgren, Adelman & Robinson 1994; Wahlgren et al. 1995; Proffitt et al. 1999). The elemental abundances are given relative to the solar system values. The solar isotope ratios by Anders & Grevesse (1989) were used.

In general the theory of radiatively driven diffusion describes the observed abundances of elements adequately. For the line–rich metals the expelling radiative force highly exceeds gravity, being thus the dominating factor in the formation of observed metal overabundances in the CP stellar atmospheres. However, essential discrepancies between the observed isotopic anomalies and the predictions of the theory still remained. The attempts to explain the observed isotope mixtures in the framework of widely used fractionation model (White et al. 1976) encounter serious difficulties (Bohlender, Dworetsky & Jomaron 1998; Hubrig, Castelli & Mathys 1999; Proffitt et al. 1999; Smith 1997; Woolf & Lambert 1999).

The situation changes essentially when an additional diffusion mechanism, called the light–induced drift (LID), is taken into account. Atutov and Shalagin (1988) discovered the effect in laboratory physical experiments as a selective acceleration of atomic particles in spectral lines by monochromatic laser beams. The importance of LID mechanism in segregation of elements and their isotopes in CP stellar atmo-

Correspondence to: Anna Aret, aret@aai.ee

 0044-6337/02/32301-0021 $ 17.50+.50/0

Table 1. The adopted parameters of HgMn stars

	HR7775	χ Lup A	
T_{eff}	10 750	10 650	
$\log g$	4.00	3.9	
$V \sin i$ (km/s)	2	0	
[Hg/H]	+5.2	+5.0	
[Mn/H]	+0.8	+0.3	
[Pt/H]	+4.7	+4.2	
[Au/H]	+3.8	+4.6	
Isotopic composition, %			Solar
Hg204	61.7	98.8	6.87
Hg202	37.2	1.1	29.89
Hg201	0.4	0.1	13.18
Hg200	0.3	–	23.10
Hg199	0.2	–	16.87
Hg198	0.2	–	9.97

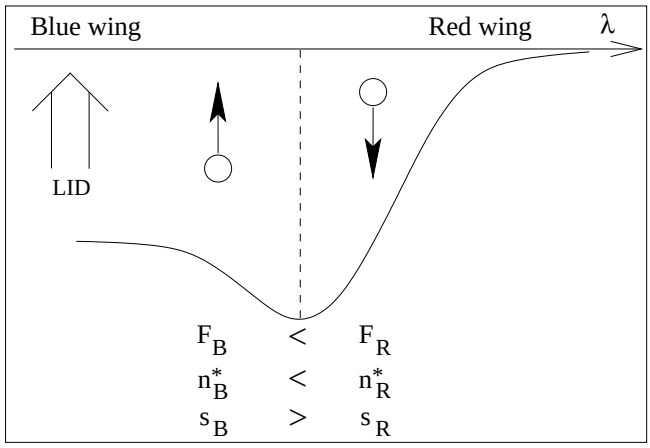

Fig. 1. Scheme of the LID generation. The arrows show the direction of thermal motion of particles absorbing radiative flux at a given frequency. In the present case particles in the blue wing of the spectral line absorb less flux and have larger free path giving thus diffusion in the direction of motion of these particles, i.e. upward.

spheres was proposed in papers by Atutov & Shalagin (1988) and Nasyrov & Shalagin (1993).

The theory for study of LID which is given in the present paper was derived by Sapar & Aret (1995) and improved in the paper by Aret & Sapar (1998). We generalized the theory of LID for the case if, in addition to the Doppler line profile also the Lorentz damping is taken into account, i.e. for the Voigt profile. Also some additional refinements, which are essential for LID in stellar atmospheres, have been made. Here we give a short review of the input physics to the LID mechanism in stellar atmospheres and study both the usual radiative acceleration and the effective radiative acceleration due to the LID on the mercury isotopes in the quiescent atmospheres of CP stars.

2. Light-induced drift (LID)

2.1. Physics of the LID

Let us consider absorption in a spectral line with asymmetrical wings (due to overlapping with a line of some other element or due to a local slope of continuum). As a result of this asymmetry there appears also asymmetry in the excitation rates of atoms and ions with different thermal Doppler shifts.

If the flux in the red wing F_R is larger than the flux in the blue wing F_B (Fig. 1) of the spectral line, there will be more excited downward–moving ions in the atmosphere than upward–moving. The collision cross–section is larger for atomic particles in the excited (upper) states than in the ground (lower) state. If the mean collision cross–section is σ , the mean thermal relative velocity of colliding particles is v_T and n is the number density of the buffer gas then the collision frequency is given by $C = n\sigma v_T$. In Fig. 1 the free paths of particles moving downward s_R are shorter than the ones of particles moving upward s_B, causing thus an upward flow of particles. Such a phenomenon of generation of flow due to anisotropic friction is called the light-induced drift. If LID is studied for small admixture elements then elastic collisions only with hydrogen and helium atoms are to be taken into account. The direction of drift depends on the flux asymmetry in the spectral line: the larger flux in the red wing produces the upward drift, the larger flux in the blue wing — the downward drift.

Isotopes with slightly shifted energy levels have overlapping spectral lines, giving systematically similar asymmetry in line profiles. Thus, the LID is most effective for diffusive segregation of isotopes. Consider, for example, a heavy element with only two isotopes. Its lighter isotope has the blueward spectral lines and the heavier isotope has the redward ones. As a result, one isotope induces a drift of another. The lighter isotope with a larger flux in the blue wing drifts downward and the heavier isotope with a larger flux in the red wing drifts upward. For light elements (say, for He) the isotopic line shift and thus the LID directions are opposite. This means that the overabundance of ^{3}He isotope and of the heaviest isotopes of Hg, Pt and some other heavy elements would be expected. For light elements the isotopic shift of spectral lines is due to the mass effect, meaning that the binding energy increases with the nuclear mass. For heavy elements this effect is essentially overweighed by the volume effect of atomic nuclei giving for heavier isotopes decreasing ionization energies and thus the isotope shifts of the spectral lines in the opposite direction compared with the light elements. The isotopic shifts are the largest ones for hydrogen and helium. LeBlanc and Michaud (1993) studied the LID for HeI isotopes in spectral line at 584 Å. Based on the LID acceleration found in the line they tried to estimate the total acceleration. They found that LID reduces the time needed for diffusion to create isotope anomalies of He. Rough estimates based on LID in single resonance lines were made also for lithium, oxygen and mercury.

2.2. Equations for LID

Let the lower state of atomic particle be l and the upper bound state u. In the result of photon absorption the radiation flux acts on particles in state u with force density

$$f_{ul}^r = \frac{\pi}{c} \int_{-\infty}^{+\infty} n_l \, \sigma_{ul}^0 W(u_\nu, a) \, F_\nu \, d\nu \; , \tag{1}$$

where πF_ν is the total monochromatic flux, n_l – the number density of particles in state l and σ_{ul}^0 — the cross–section of photon absorption in transition $l \rightarrow u$, which can be expressed using oscillator strength f_{ul} in the form

$$\sigma_{ul}^0 = \frac{\pi \, e^2 f_{ul}}{m_e c \, \Delta\nu_D} \; , \tag{2}$$

where $\Delta\nu_D$ is the Doppler width of spectral line.

The normalized frequency distribution in a spectral line is the Voigt function, being the convolution of the Lorentz and Doppler profiles, i.e.

$$W(u_\nu, a) = \int_{-\infty}^{\infty} W(u_\nu, a, y) dy \; , \tag{3}$$

where the integrand of the Voigt function

$$W(u_\nu, a, y) = \frac{a}{\pi^{3/2}} \frac{e^{-y^2}}{(u_\nu - y)^2 + a^2} \; . \tag{4}$$

The argument of the Voigt function is the dimensionless frequency $u_\nu = (\nu - \nu_0)/\Delta\nu_D$, its parameter is the ratio of characteristic widths of Lorentz and Doppler profiles, $a = \Gamma_{ul}/(4\pi\Delta\nu_D)$ and integration is carried out over the dimensionless velocity $y = v/v_T$, where the thermal velocity $v_T = \sqrt{2kT/M}$ and M is the mass of the light–absorbing ion.

Light–induced drift can be generated in spectral lines only due to difference of elastic collision cross–sections in different quantum states. For spectral lines the cross–section of the upper state of transition σ_u is larger than the one of the lower state σ_l because the cross–sections of elastic collisions can be well approximated using the effective radius r_i found using the ionization energy E_i of the state i from classical expression $Ze^2/r_i = E_i$. This means that the free path of atomic particles in upper state is shorter than in the lower state. Collisions of atoms or of an atom and an ion are predominately elastic. Elastic collisions give also a small additional contribution to the Coulomb interaction of ions. We assume complete thermalization of particle motion in collisions, which gives maximal effect of light–induced drift. Based on the above described features of particle interaction in CP stellar atmospheres we obtain for the ratio of free paths

$$\frac{s_u}{s_l} = \frac{\sigma_l}{\sigma_u} = \frac{C_l}{C_u} \; , \tag{5}$$

where C is the collision frequency for particles in the quantum state given by subscript. The effective braking rate for particles in the upper state is

$$\beta = \frac{s_l - s_u}{s_l} = 1 - \frac{C_l}{C_u} \; . \tag{6}$$

Between two consequent collisions of atomic particles spontaneous radiative electron transitions take place. This reduces the LID efficiency by factor

$$\alpha = \frac{C_u}{A_u + C_u} \; , \tag{7}$$

where A_u is the frequency (probability) of spontaneous transitions from the upper state. Taking into account that the role of induced de-excitation is low we have ignored the term.

The total efficiency of LID mechanism due to both these factors is thus

$$D = \alpha\beta = \frac{C_u - C_l}{A_u + C_u} \; . \tag{8}$$

The essence of LID is that particles of given species can have different free paths in different directions. The situation appears in stellar atmospheres in the presence of asymmetric flux in the blue and red wings of spectral line profile. In this case particles moving upward and downward have different free paths. These circumstances lead to the light–induced drift phenomenon.

The LID starts with radiative excitation of an atomic particle from a lower state to an upper state. Let $F_\nu(\mu)$ be the radiative flux in the direction specified by $\mu = \cos\vartheta$. The number of radiative flux induced excitations per unit volume and unit time interval is proportional to the number density of particles n_l, the number of photons in flux $\pi F_\nu(\mu)/h\nu$ and the photon absorption cross–section in line $\sigma_{ul}^0 W(u_\nu, a, y)$ at frequency ν. The usual radiative force is generated by the photon momentum $h\nu/c$ transferred to radiation absorbing atomic particle. The effective force generated by LID is obtained replacing the photon momentum by the uncompensated part D of thermal Doppler momentum of particles in the lower state. This momentum is directed oppositely to the moment of particles absorbing flux, i.e. it is expressed by $-DMv$. Thus, integrating over photon frequencies, thermal Doppler velocities and directions we obtain

$$f_{ul}^D = \tag{9}$$
$$- D \int_0^{+\infty} d\nu \int_{-\infty}^{+\infty} dy \int_0^1 d\mu \, n_l M v \sigma_{ul}^0 W(u_\nu, a, y) \frac{\pi F_\nu(\mu)}{h\nu} .$$

Taking into account that $v = v_T y$ we obtain from Eqs.(3) and (4)

$$\partial W(u_\nu, a)/\partial u_\nu = -2 \int_{-\infty}^{+\infty} y W(u_\nu, a, y) dy \; . \tag{10}$$

Thus we can reduce the expression (10) for the force density to the form

$$f_{ul}^D = qD \frac{\pi}{c} \int_0^{+\infty} n_l \sigma_{ul}^0 \frac{\partial W(u_\nu, a)}{\partial u_\nu} F_\nu d\nu \; , \tag{11}$$

where $q = \dfrac{Mv_T}{2} \dfrac{c}{h\nu}$.

The total effective force on atomic particle due to both the radiative force and the LID is given by $f_{ul}^t = f_{ul}^r + f_{ul}^D$. Thus, the effect of the light–induced drift can be incorporated by

replacing the Voigt function $W(u_\nu, a)$ in the radiative force expression Eq.(1) by

$$w(u_\nu, a) = W(u_\nu, a) + qD\frac{\partial W(u_\nu, a)}{\partial u_\nu} \ . \tag{12}$$

From these formulae it follows that the LID can be treated as an additional specific force. Excellent analysis of the Voigt function and the FORTRAN computer codes for both the Voigt function and its derivative are given by J. Humlíček (1979).

Let us show that our formula for LID (Eq.(11)) reduces to the same form as Eq.(1) for the LID velocity by Atutov and Shalagin (1988). The LID velocity can be expressed in the form

$$v^D = \frac{a^D}{C_l} = \frac{f_{ul}^D}{C_l M n_l} \ . \tag{13}$$

The Einstein coefficient A_u and the oscillator strength f_{ul} are connected by $f_{ul} = A_u/3\gamma_{cl}$, where γ_{cl} is classical dumping constant. Thus, the Eq.(2) takes the form

$$\sigma_{ul}^0 = K_\sigma A_u \ , \quad \text{where } K_\sigma = \frac{\pi e^2}{3\gamma_{cl} m_e c \Delta\nu_D} \ . \tag{14}$$

From Eq.(11) it follows

$$v^D = v_T D \frac{A_u}{C_l} K_\sigma \Delta N \ , \tag{15}$$

$$\text{where } \Delta N = \frac{1}{2}\int_0^{+\infty} \frac{\partial W(u_\nu, a)}{\partial u_\nu}\frac{\pi F_\nu}{h\nu} d\nu \ .$$

Taking into account Eq.(8) for the correction factor D we find for the LID velocity the expression

$$v^D = v_T \frac{C_u - C_l}{C_l}\frac{A_u}{A_u + C_u} K_\sigma \Delta N \ , \tag{16}$$

which practically coincides with that of Atutov and Shalagin (1988).

Let us estimate now the efficiency of LID in stellar atmospheres. The ratio of the mean thermal momentum of atomic particle Mv_T to the momentum of absorbed photon $h\nu/c$ is about 10^4. That is why the LID is important even in the case of moderate asymmetry of radiative flux in the spectral line profiles.

The value of D can be found only with rather low exactness. For rough estimates we may take $A_u = 10^8\, s^{-1}$, for outer layers of the CP star atmospheres $C_u = 10^6\, s^{-1}$ and for deeper layers $C_u = 10^8\, s^{-1}$. If for rough estimates we accept that $C_l/C_u = 1/2$, then in this approximation the characteristic values of the correction factor D are about $5 \cdot 10^{-3}$ in the outer atmospheric layers of the CP stars and about 0.25 in the deeper layers. Thus, the effective value of qD reduces to 20 in the outer atmospheric layers and conserves large values in the deeper layers. In model computations we used the values of quantity D calculated using the quasi–classical formulae for cross–sections and quantum state life–times.

3. Computations

Together with R. Poolamäe we have composed a new FORTRAN computer code for computation of synthetic stellar spectra. Using the software we computed the accelerations due to usual radiative force and due to LID for some chemical elements and their isotopes in the atmospheres of the CP stars. In the computer code we used approximately the same input physics as used by R. Kurucz (1993) and given on his CD–ROM18 for computing synthetic spectra. The code composed by us and Poolamäe is several times shorter than the computer codes by Kurucz and it is written as a single file with additional include file for COMMONs. The program incorporates also somewhat modified Kurucz codes for computation of radiative transfer.

Accelerations for mercury isotopes (Hg 198, 199, 200, 201, 202, 204), for iron and manganese have been calculated using the Kurucz (1993) model stellar atmosphere with $T_{eff} = 10750$ K, $\log g = 4$ and $v \sin i = 0$. Three different abundances of mercury were used: solar abundance (the total mercury abundance $\log N(\mathrm{Hg}) = -10.96$, where $\log N(\mathrm{H}) = 0$), solar abundance + 5 dex (both with the solar mixture of isotopes) and the HR7775 isotope mixture given in Table 1. The Kurucz CD–ROM18 (Kurucz 1993) line lists have been used. The number of used HgI spectral lines was 27 including 2 resonance lines and the number of HgII spectral lines was 31 including 5 resonance lines. The lines used cover the spectral interval from 800 to 12 000 Å. As expected, the results of our computations show that the dominant contribution in the LID is given by resonance lines.

We adopted the relative isotope shifts as the mean values found by Striganov & Dontsov (1955), namely $[202-200] = 1$, $[198-200] = -0.94$, $[199-200] = -0.80$, $[201-200] = 0.30$, $[204-200] = 1.98$. For scaling these relative shifts to wavenumbers, we have taken into account that $[202-200] = 0.179\,\mathrm{cm}^{-1}$ for HgI and $[202-200] = 0.508\,\mathrm{cm}^{-1}$ for HgII.

The computations were carried out with constant frequency step $\Delta\nu/\nu = 1/R$ taking for the computational resolution value $R = 5 \cdot 10^6$. Such a high resolution is needed because spectral lines of mercury are narrow and their isotopic shifts are small. We emphasize that for isotope segregation we need very exact data both for isotope splitting of spectral lines and for the spectral lines overlapping with them.

4. Results

4.1. Solar abundance and solar isotopic mixture of mercury

The effective acceleration on mercury isotopes due to the LID cannot *a priori* be expected to be large in the case of solar abundances of isotopes because blending with strong neighboring lines is more important than mutual influence of very weak lines of mercury isotopes. However, it turned out that for ^{198}Hg acceleration due to the LID exceeds to 3 dex the radiative acceleration (Fig. 2). The acceleration is directed downward for ^{198}Hg, ^{199}Hg, ^{202}Hg and ^{204}Hg and upward for ^{200}Hg and Hg^{201}. As a result, the abundances of sinking

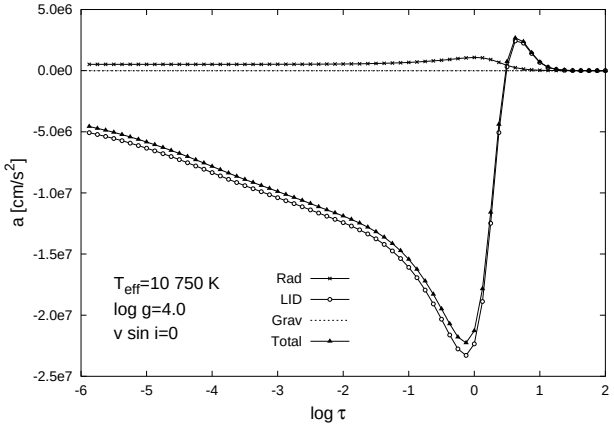

(a) Radiative acceleration, LID and gravity.

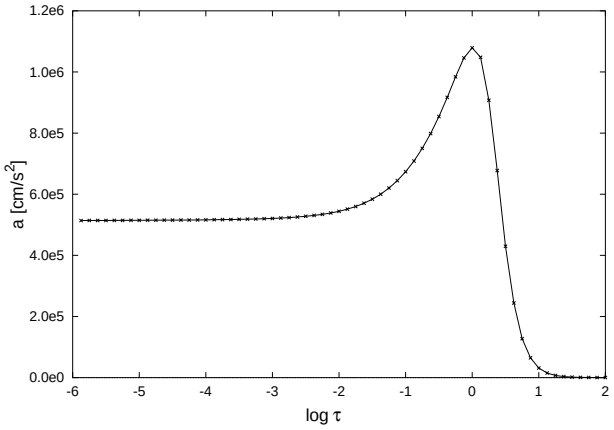

(b) Radiative acceleration.

Fig. 2. Acceleration on ^{198}Hg ions due to radiative force, LID and gravity for the case if mercury abundance and its isotope ratios are solar.

Hg isotopes in deep atmospheric layers increase drastically. This happens due to the circumstance that the role of HgI and HgII in these layers diminishes strongly, resulting in steep and drastic lessening of the computed LID acceleration. Accumulation of isotopes ^{202}Hg, ^{204}Hg will turn the sinking (sedimentation) of ^{204}Hg into rising (levitation) as it is the case for the metal–rich CP stars analyzed below.

The isotopes ^{198}Hg and ^{199}Hg have in the case of solar abundances a strong downward drift, having maximum at about τ=1 and decreasing steeply at larger Rosseland optical depths. As a general feature, starting from about τ=10 effective acceleration due to the LID is low.

4.2. High abundance of mercury (solar + 5 dex) and solar isotopic mixture

The situation is drastically different in the model atmosphere with high mercury abundance (solar + 5 dex). The mercury lines in such an atmosphere are strong and the mutual influence of overlapping isotope lines is dominant (Fig. 3), generating large light–induced drift. Effective acceleration due to the LID exceeds radiative acceleration up to 2 dex, determining the total acceleration of mercury isotopes. As expected, the accelerations of three lighter isotopes (^{198}Hg, ^{199}Hg, ^{200}Hg) are directed downward and the accelerations of three heavier isotopes (^{201}Hg, ^{202}Hg, ^{204}Hg) are directed upward. Both the downward and upward directed accelerations reach maximum absolute value at about τ=1 and diminish drastically at $\tau \approx$100. The acceleration curve for ^{198}Hg is shown in Fig. 4, the curves for ^{199}Hg and ^{200}Hg are generally similar but accelerations are about 3 and 9 times smaller, correspondingly. The acceleration curves for three heavier isotopes have similar features, the acceleration of ^{204}Hg is the largest (Fig. 6), its values for ^{202}Hg (Fig. 5) and ^{201}Hg are smaller about 3 and 9 times, respectively. Thus, in the mercury–rich atmospheres the LID causes sinking of lighter isotopes and rising of heavier ones, leading to the segregation of isotopes.

4.3. HR7775 abundance and isotopic mixture of mercury

In the atmosphere of HR7775 the abundance of mercury exceeds solar abundance by 5.2 dex, at the same time the isotope ratios differ drastically from the solar ones (Table 1). As a result of segregation of isotopes only the two heaviest isotopes remained and are dominating in the line profile formation (Fig. 7). The segregation due to the LID continues. The lighter of these isotopes ^{202}Hg, which rises in the atmosphere with solar mixture of isotopes (Fig. 5) now sinks (Fig. 8). The LID acceleration exceeds the gravity about 1.5 dex. Thus, accumulation of ^{204}Hg continues in the upper layers of HR7775 (Fig. 9).

4.4. Iron and manganese

The LID turned out to be important for line–rich elements even when isotopic splitting of spectral lines is ignored. We have obtained this preliminary result computing accelerations for iron and manganese for model atmosphere with solar abundances of elements. All iron and mercury lines given in the Kurucz CD-ROM18 line lists have been included. The contribution by the LID to total acceleration for both elements turned out to be on an average of the same order of magnitude as the contribution by the usual radiative force.

4.5. Conclusions

Based on our results we may conclude that isotopic composition in mercury–manganese stars evolves from solar mixture to mixture in HR7775 and further to extreme isotopic structure of χ Lup. The most complicated are the early stages of isotope segregation when mercury abundance is close to the solar value. Blending of weak mercury lines with strong lines of other elements turns out to be then more important than mutual blending of mercury isotope lines. This circumstance makes computed isotope accelerations very sensitive to line data.

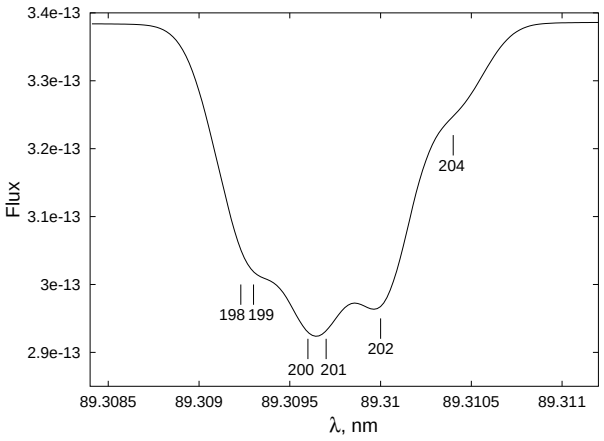

(a) Hg II resonance line $6s^2S_{1/2} \rightarrow 7p^2P_{3/2}$

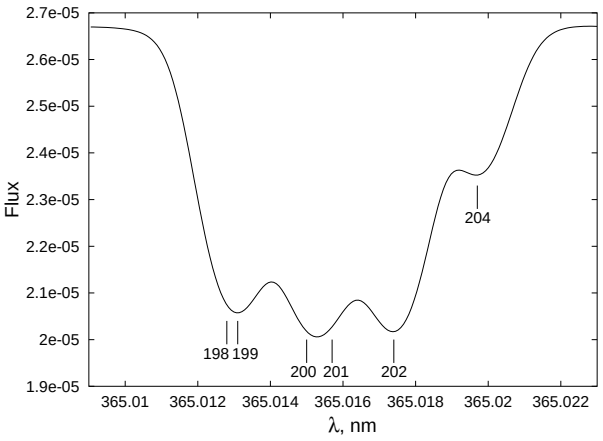

(b) Hg I line $6p^3P_2 \rightarrow 6d^3D_3$

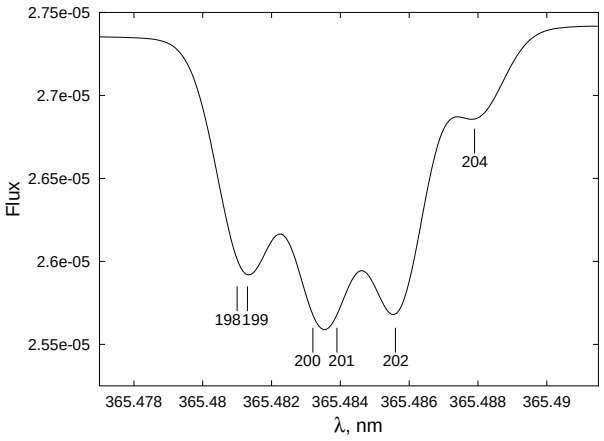

(c) Hg I line $6p^3P_2 \rightarrow 6d^3D_2$

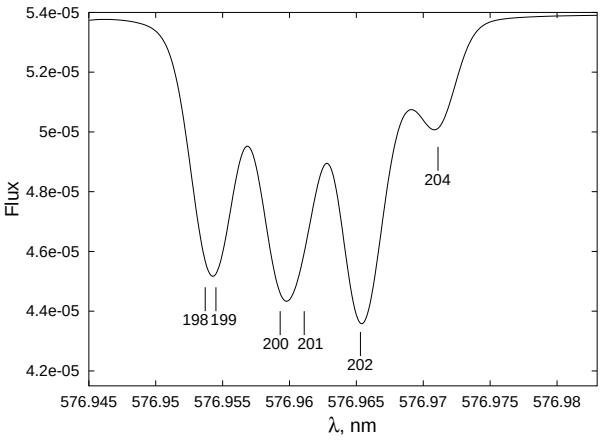

(d) Hg I line $6p^1P_1 \rightarrow 6d^3D_2$

Fig. 3. Mercury lines in model atmosphere $T_{eff} = 10750$ K; $\log g = 4.0$; $v \sin i = 0$. Hg abundance: solar + 5 dex, solar isotope ratios.

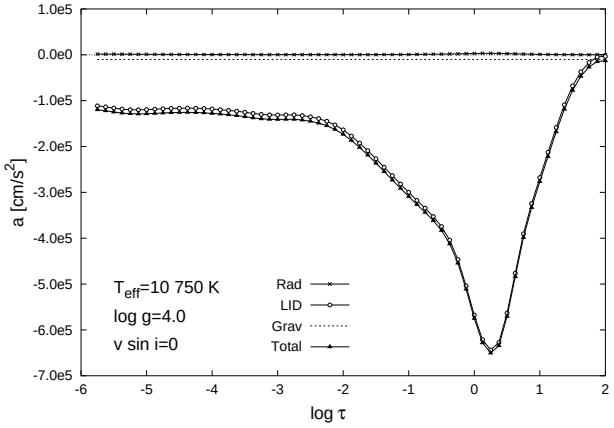

(a) Radiative acceleration, LID and gravity.

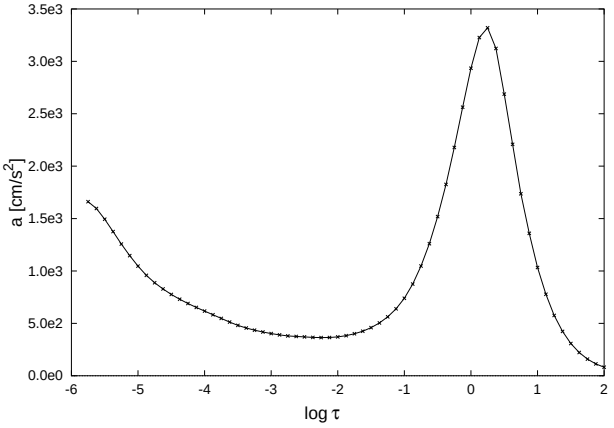

(b) Radiative acceleration.

Fig. 4. Acceleration on ^{198}Hg due to radiative force, LID and gravity. Hg abundance: solar + 5 dex, solar isotope ratios.

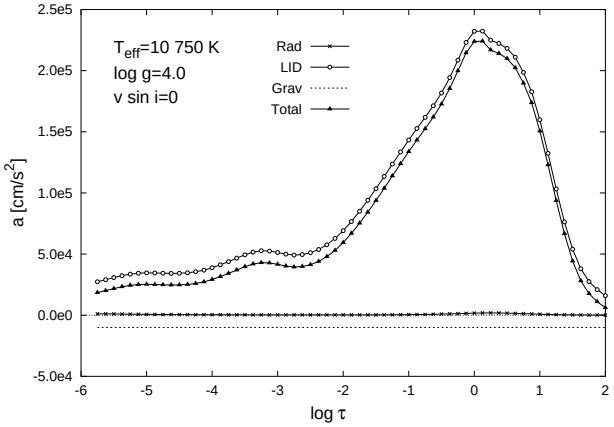

(a) Radiative acceleration, LID and gravity.

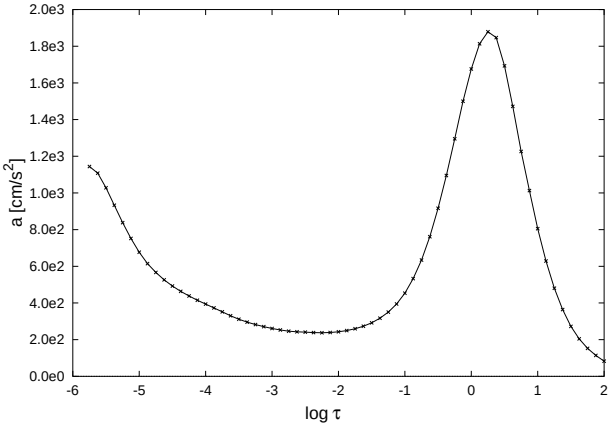

(b) Radiative acceleration.

Fig. 5. Acceleration on ^{202}Hg due to radiative force, LID and gravity. Hg abundance: solar + 5 dex, solar isotope ratios.

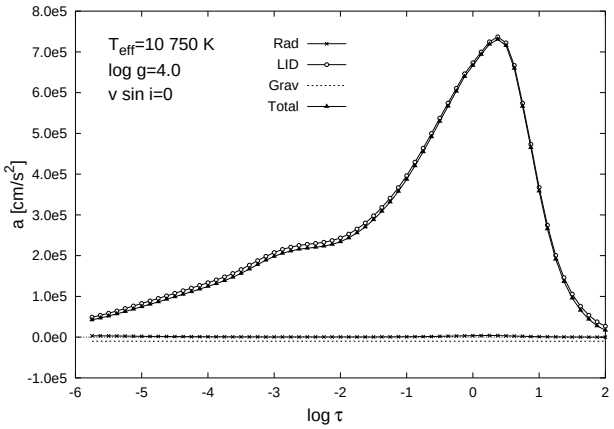

(a) Radiative acceleration, LID and gravity.

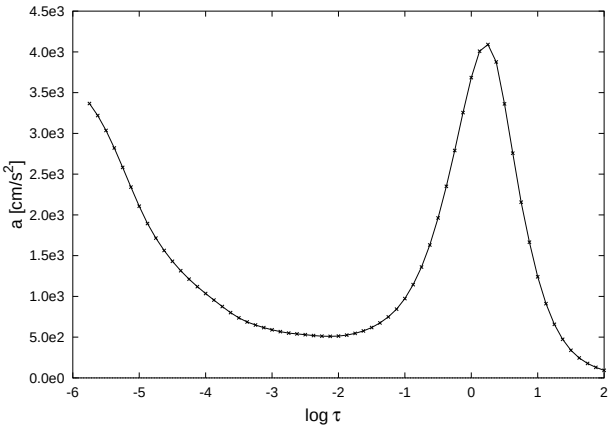

(b) Radiative acceleration.

Fig. 6. Acceleration on ^{204}Hg due to radiative force, LID and gravity. Hg abundance: solar + 5 dex, solar isotope ratios.

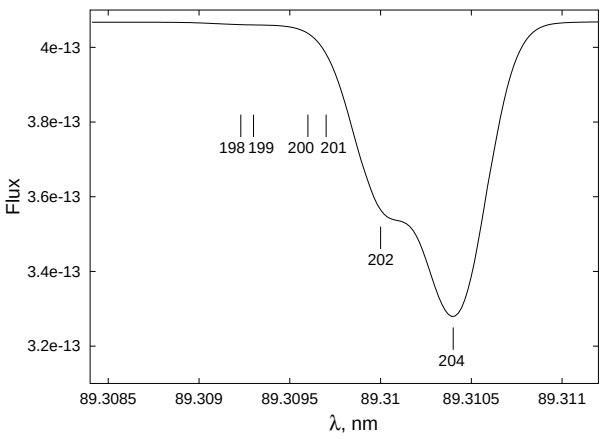

(a) Hg II resonance line $6s^2S_{1/2} \rightarrow 7p^2P_{3/2}$

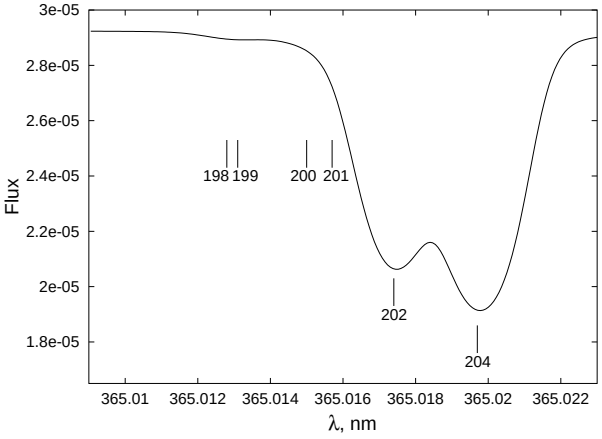

(b) Hg I line $6p^3P_2 \rightarrow 6d^3D_3$

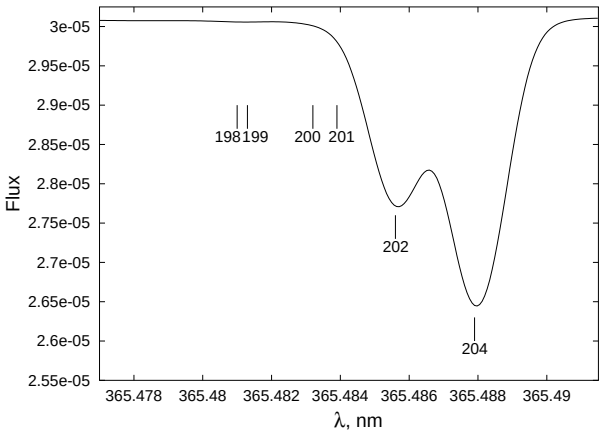

(c) Hg I line $6p^3P_2 \rightarrow 6d^3D_2$

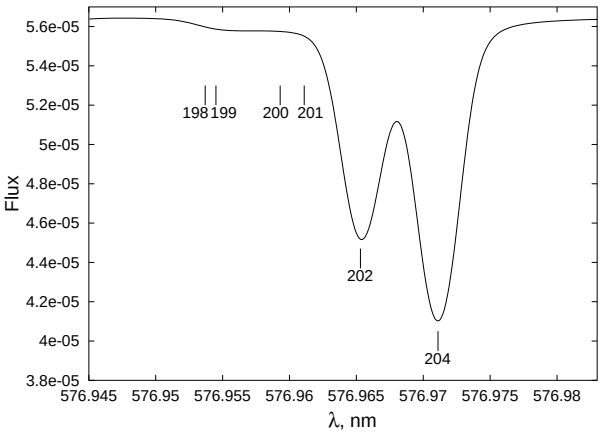

(d) Hg I line $6p^1P_1 \rightarrow 6d^3D_2$

Fig. 7. Mercury lines in model atmosphere $T_{eff} = 10750$ K; $\log g = 4.0$; $v \sin i = 0$. Hg abundance: solar + 5.2 dex, HR7775 isotope ratios.

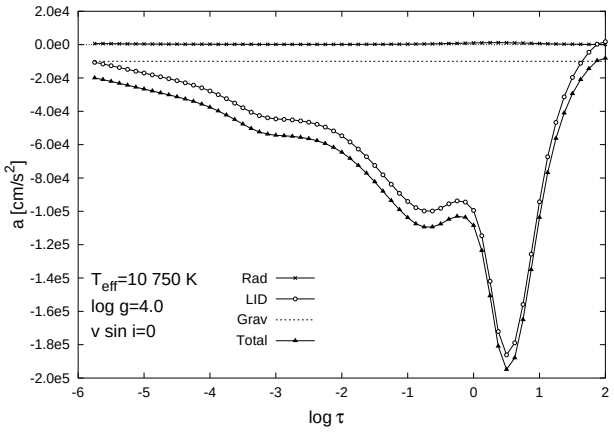

(a) Radiative acceleration, LID and gravity.

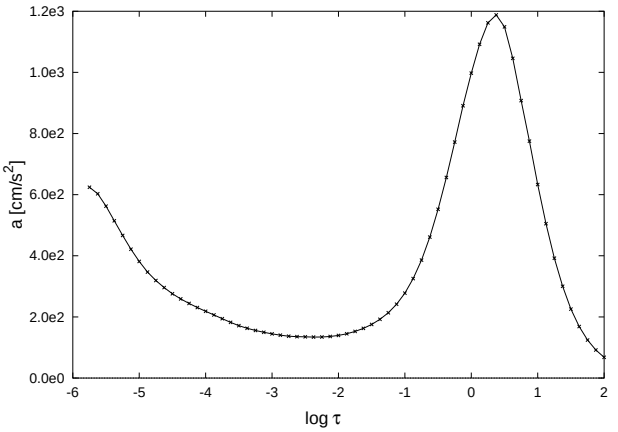

(b) Radiative acceleration.

Fig. 8. Acceleration on ^{202}Hg due to radiative force, LID and gravity. Hg abundance: solar + 5.2 dex, HR7775 isotope ratios.

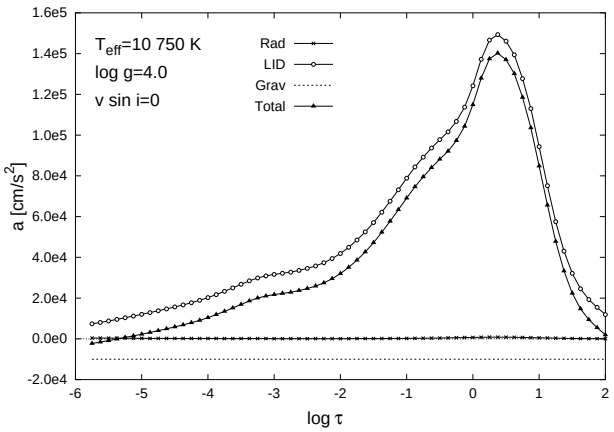

(a) Radiative acceleration, LID and gravity.

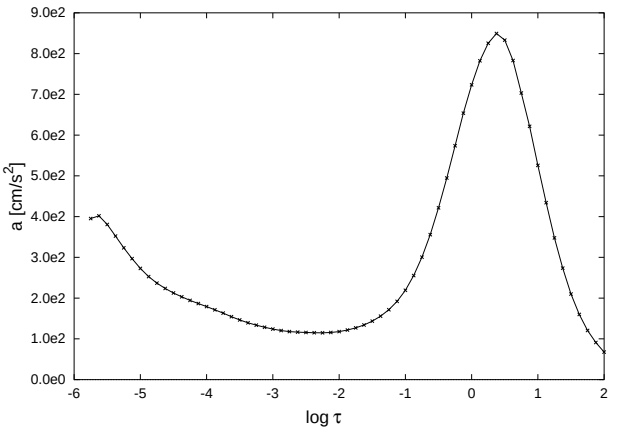

(b) Radiative acceleration.

Fig. 9. Acceleration on ^{204}Hg due to radiative force, LID and gravity. Hg abundance: solar + 5.2 dex, HR7775 isotope ratios.

Summing up, the light–induced drift is important to be taken into account in the evolutionary calculations of diffusion of elements and their isotopes in the atmospheres of the CP stars. It is important to emphasize that such computations give for elements and their isotopes the abundance distribution throughout the CP star atmospheres.

5. Discussion

Computations of isotope segregation need extremely high spectral resolution, exact and complete line databases, where the isotopic and hyperfine splitting must be taken into account. The present databases are inadequate in this aspect and must be completed in further studies. The values of collision cross–sections need to be improved.

The LID is much smaller for ionized than for neutral elements since the dominating component of the collision cross–section for an ionized particle is the Coulomb cross–section which is almost the same in the excited and in the ground state. The effective cross–section of two colliding charged particles is about 2 dex larger than that of two colliding neutral particles or a neutral particle and an ion. This circumstance reduces the efficiency of the LID for ions almost proportionally to the mean degree of ionization.

We have started further study of evolutionary segregation of the chemical elements and their isotopes in the quiescent stellar atmospheres, which leads to formation of CP stars. For the computations the model accelerations for each element and its isotope are to be used in the equations of diffusive segregation. The abundances of chemical elements and of their isotopes undergo different evolutionary changes in different layers of stellar atmosphere. Thus, computation of new values of acceleration corresponding to the current chemically inhomogeneous atmospheres must be carried out. Characteristic abundances of CP stars are forming on the time scale of millions of years. However, the time scale estimate may need essential correction in the direction of longer ages of CP stars due to presence of weak stellar winds, slow turbulence and meridional circulation in the slowly rotating stars. All these effects, if they are present, diminish the efficiency of diffusion processes. Also presence of magnetic field can modify the evolutionary scenarios.

Acknowledgements. We are thankful to R. Kurucz for providing us with his CDs with computer codes and line data files, R. Poolamäe for his contribution in composing the software and Estonian Science Foundation for support by grants No. 2629 and 4701. We are also thankful to J. Kubát and a referee for their stimulating remarks.

References

Adelman, S.J.: 1994, Mon. Not. R. Astron. Soc. 226, 97
Anders, E., Grevesse, N.: 1989, Geochim. Cosmochim. Acta 53, 197
Aret, A., Sapar, A.: 1998, Contr. Astron. Obser. Skalnaté Pleso 27, 329
Atutov, S.N., Shalagin, A.M.: 1988, Soviet Astron. Lett. 14, 285
Bohlender, D. A., Dworetsky, M. M., Jomaron, C. M.: 1998, Astrophys. J. 504, 533
Cowley, C.R., Aikman, G.C.L.: 1975, Publ. Astron. Soc. Pac. 87, 513
Hubrig, S., Castelli, F., Mathys, G.: 1999 Astron. Astrophys. 341, 190
Humlíček, J.: 1979, J. Quant. Spectrosc. Radiat. Transfer 21, 309
Jomaron, C.M., Dworetsky, M.M., Bohlender, D.A.: 1998, Contr. Astron. Obser. Skalnaté Pleso 27, 324
Kalus, G., Johansson, S., Wahlgren, G.M., Leckrone, D.S., Thorne, A.P., Brandt, J.C.: 1998, Astrophys. J. 494, 792
Kurucz, R.: 1993, SYNTHE Spectrum Synthesis Programs and Line Data. Kurucz CD-ROM No. 18. Cambridge, Mass.: Smithsonian Astrophysical Observatory
LeBlanc, F., Michaud, G.: 1993, Astrophys. J. , 408, 251
Leckrone, D.S., Johansson, S., Kalus, G., Wahlgren, G.M., Brage, T., Proffitt, C.R.: 1996, Astrophys. J. 462, 937
Michaud, G.: 1970, Astrophys. J. 160, 641
Nasyrov, K. A., Shalagin, A. M.: 1993, Astron. Astrophys. 268, 201
Proffitt, C.R., Brage, T., Leckrone, D.S., Wahlgren, G.M., Brandt, J.C., Sansonetti, C.J., Reader, J., Johansson, S.G.: 1999, Astrophys. J. 512, 942
Sapar, A., Aret, A.: 1995, Astron. Astrophys. Trans. 7, 1
Smith, K.C.: 1993, Astron. Astrophys. 276, 393
Smith, K.C.: 1994, Astron. Astrophys. 291, 521
Smith, K.C.: 1996a, Astrophys. Sp. Sci. 237, 77
Smith, K.C.: 1996b, Astron. Astrophys. 305, 902
Smith, K.C.: 1997, Astron. Astrophys. 319, 928
Smith, K.C., Dworetsky, M.M.: 1993, Astron. Astrophys. 274, 335
Striganov, A.R., Dontsov, Yu.P.: 1955, Uspekhi Fizicheskikh Nauk 55, 315 (in Russian)
Wahlgren, G.M., Adelman, S.J., Robinson, R.D.: 1994, Astrophys. J. 434, 349
Wahlgren, G.M., Leckrone, D.S., Johansson, S.G., Rosberg, M., Brage, T.: 1995, Astrophys. J. 444, 438
White, R.E., Vaughan, A.H., Preston, G.W., Swings, J.P.: 1976, Astrophys. J. 204, 131
Wolff, S.C., Preston, G.W.: 1978, Astrophys. J. Suppl. 37, 371
Woolf, V.M., Lambert, D.L.: 1999 Astrophys. J. 521, 414